A GLOBAL MAGNETOHYDRODYNAMIC SIMULATION OF MAGNETOSPHERIC DYNAMICS WHEN THE IMF IS SOUTHWARD: MAPPING TO THE AURORAL ZONE

Raymond J. Walker[1], Tatsuki Ogino[2], Maha Ashour-Abdalla[1,3], and Joachim Raeder[1]

[1] Institute of Geophysics and Planetary Physics, University of California, Los Angeles, CA 90024–1567
[2] Solar Terrestrial Environment Laboratory, Nagoya University, Toyokawa, Japan
[3] Physics Department, University of California, Los Angeles, CA 90024–1547

ABSTRACT

We have used a new high resolution global magnetohydrodynamic simulation model to investigate magnetospheric dynamics during intervals with southward interplanetary magnetic field (IMF). When the southward IMF reaches the dayside magnetopause reconnection begins and magnetic flux is convected into the tail lobes. After about 35m reconnection begins within the plasma sheet near midnight at $x = -14R_E$. Later the x-line moves towards the magnetopause. The reconnection occurs just tailward of the region where the tail attaches onto the dipole dominated inner magnetosphere. Later when all the plasma sheet field lines have reconnected a plasmoid moves down the tail. We also have calculated the region of the ionosphere where the energy flux from the magnetosphere is greatest. The energy flux is confined to a region which approximates the auroral oval.

1. INTRODUCTION

It has long been recognized that the Interplanetary Magnetic Field (IMF) orientation controls magnetospheric dynamics (see McPherron, (Ref. 1) for a recent review). Magnetospheric substorms are associated with a southward IMF and most models of substorm dynamics start with dayside reconnection. The most frequently discussed model is the near earth neutral line model. However this model is not universally accepted. Other models include the driven model (Refs. 2, 3), the boundary layer dynamics model (Ref. 4) and the thermal catastrophe model (Refs. 5, 6). The models differ most in their dependence on the physics in the near earth $x > -40R_E$ part of the magnetotail.

In the near earth neutral line model the onset of dayside merging is not immediately followed by an increase in reconnection at the distant neutral line in the magnetotail. Instead flux accumulates in the tail lobes. This leads to a distortion of the magnetosphere in which the tail current sheet moves inward and the current increases while the plasma sheet thins. Tearing mode reconnection then begins in a localized part of the plasma sheet on closed field lines forming an x-type neutral line and an o-type neutral line. The expansion phase of the substorm begins when all of the closed plasma sheet field lines have reconnected and reconnection starts on open tail lobe field lines. This is thought to occur explosively. The tension on the lobe magnetic field lines which drape over the o–line pull it tailward.

In this paper we present the results of a new calculation of the response of the tail to a southward IMF by using a global MHD model. Our emphasis is on the onset of the substorm process and on mapping phenomena between the ionosphere and the magnetosphere. In section 2 we describe the latest version of our global MHD code. The results from the simulation of the temporal evolution of the magnetosphere when the IMF is southward are presented in section 3 while in sections 4 and 5 we present the results of our mapping studies. Finally in section 6 we summarize these results in the context of previous theories and observations.

2. THE SIMULATION MODEL

The latest version of our model has been presented in detail by Ogino et al., (Ref. 7) so we will just review its main features here. We have solved the MHD equations and Maxwell's equations as an initial value problem. The normalized resistive MHD equations are the same as those we used in our earlier simulations (Ref. 8).

In the simulation, a uniform solar wind with $n_{sw} = 5/cm^3, v_{sw} = 300km/s$ and $T_{sw} = 2 \times 10^{5o}K$ flows into a simulation box of dimensions $-48R_E \leq x \leq 24R_E, 0 \leq y \leq 24R_E$ and $0 \leq z \leq 24R_E$ at $x = 24R_E$. Free boundary conditions where the derivatives of all physical quantities are zero, were used at $x = -48R_E$, $y = 24R_E$ and $z = 24R_E$. At $y = 24R_E$ and $z = 24R_E$ the free boundary is at 45° to the x-axis. Mirror boundary conditions were used at $z = 0$ and $y = 0$. The magnetic field of the earth was taken to be an untilted dipole field.

The ionospheric boundary condition imposed near the earth was determined by requiring a static equilibrium (Ref. 8). We held all of the model parameters $(\rho, \vec{v}, P, \vec{B})$ constant for $r < 3.5R_E$. A smoothing function damps out all perturbations near the ionosphere including parallel currents.

The grid was (242,82,82) with a mesh size of $0.3R_E$ and the time step was $\Delta t = 1.12s$.

In the new code we solve the differential equations by using a modified version of the Leapfrog scheme which is a combination of the Leapfrog scheme and the two step Lax-Wendroff scheme (Ref. 7).

3. CHANGES IN THE MAGNETOSPHERIC CONFIGURATION WHEN THE IMF IS SOUTHWARD

At time $t = 0$, the southward IMF entered the simulation box at its upstream edge. In Figure 1, we have plotted magnetic field vectors $(\vec{B})$, flow vectors $(\vec{V})$, density contours (ρ) and pressure

contours (P) 38m after the southward IMF entered the simulation box. The flow, density and pressure are plotted such that the top half of the figure corresponds to the noon-midnight meridian while the bottom half of each figure includes results from the equatorial plane. The magnetic field vectors are confined to the noon-midnight meridian.

By this time reconnection has already started at the subsolar magnetopause. In the tail the plasma sheet has started to thin and has a half thickness of $\sim 2R_E$. At about $x = -14R_E$ reconnection has started within $\sim 6R_E$ of midnight. Evidence for reconnection is most clearly seen in the equatorial flows which reverse direction near midnight. Also B_z (not shown) has developed a southward component for $-14R_E > x > -21R_E$ (Ref. 9). Both the earthward and the tailward flows at midnight have a velocity of about 50km/s. The large flow cells in the equator near the tail magnetopause are viscous cells.

Also evident in Figure 1 is a plasma mantle like flow in the lobes of the tail. This flow has an equatorward component and has penetrated about half way into the lobes.

In Figure 2 we present a three dimensional view of the magnetic field configuration. The bottom panel contains field lines with at least one end attached to the earth. Here newly reconnected dayside field lines are characterized by sharp bends. The kink straightens out slowly as the field line is convected tailward. A series of such lines can be seen stretching into the magnetotail and around the dusk magnetopause. This figure demonstrates that convection is a three dimensional phenomenon even when the IMF is purely southward.

In the top panel the open field lines have been removed and magnetosheath field lines have been added. Closed field lines extend across the entire width of the plasma sheet. The only indication of the tail reconnection is a small dip in the field lines near midnight at $x = -14R_E$. The reconnection started on closed field lines. The dip is caused by the convection of closed field lines into the reconnection region.

At 47m, the plasma sheet has continued to thin (Figure 3). Now the convection in the lobes extends further into the tail but has not reached the equator in the region modeled by the simulation. The reconnection has continued and has spread across the tail. The earthward flows at midnight have remained at about 50 km/s while the tailward flows have increased to about 130 km/s. Near the magnetopause the flows from the reconnection region have a substantial V_y component as well as tailward or earthward components. They have combined with the V_y flow from the viscous cells resulting in outward motion of the magnetopause.

At the dayside magnetopause two small flow vortices have formed. Careful examination of both the flow field (Figure 1) and the magnetic field indicates that the vortices start at about 1500 LT or 1600 LT at $t = 38m$. We believe that these vortices are caused by the Kelvin-Helmholtz instability at the magnetopause. Walker et al. (Ref. 9) have shown that at $\sim 1600LT$ the velocity shear across the magnetopause ($\sim 250km/s$) equals the critical velocity for the Kelvin-Helmholtz instability. The flow from the tail reconnection to the dayside contributes ~ 80 km/s to the shear so we would not expect the boundary to be unstable to the Kelvin-Helmholtz instability in the absence of tail reconnection. When we run the simulation with a northward IMF, the vortices at the boundary do not form.

In Figure 4, a plasmoid can be seen tailward of the reconnection region. At this time reconnection is occurring on open lobe field lines all across the tail. Only a few closed field lines still drape over the plasmoid. Near midnight the plasmoid has started to move tailward. This is caused by the tension of the reconnected open field lines which now drape over the plasmoid. The plasmoid has a curved foot print in the equatorial plane be-

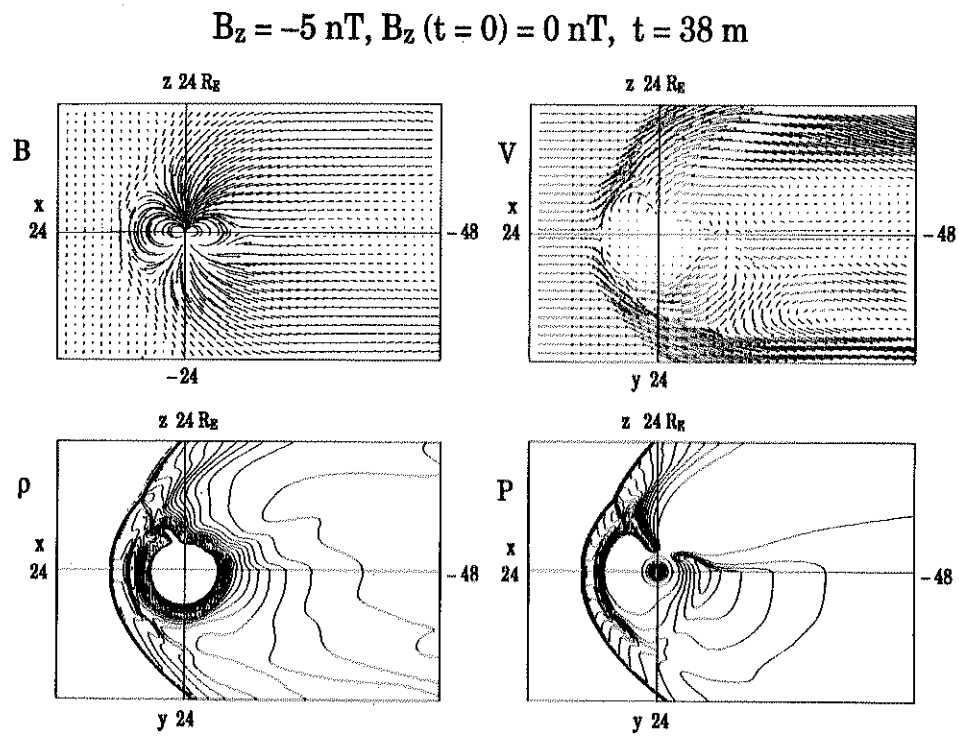

Fig. 1: Magnetic field vectors ($\vec{B}$), flow velocity vectors ($\vec{V}$), density contours (ρ) and pressure contours (P) $t = 38m$ after the start of the simulation.

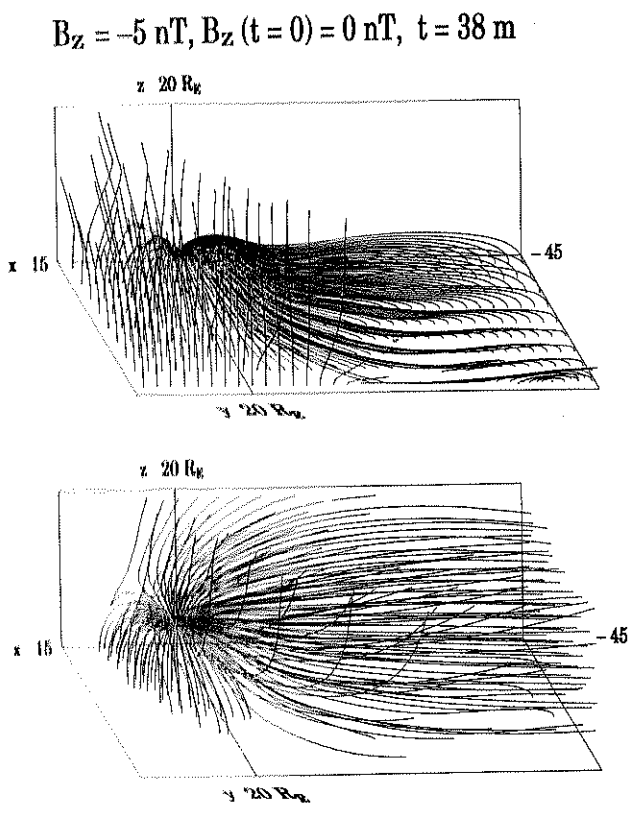

Fig. 2: Magnetic field lines at $t = 38m$.

cause it has been moving tailward near midnight for awhile but has not started to move nearer to the magnetopause.

At $t = 57m$, the reconnection continues in the near earth tail where the tailward flows are now $\sim$ 150 km/s (Figure 5). The magnetopause has continued to expand in the y direction. Unfortunately it has grown wider than the simulation box. The boundary condition at the dusk boundary was not designed for the case where the magnetopause is outside of the simulation box. While the results should not be trusted in this region, we do not think that this has effected the results in the rest of the magnetosphere since those results follow continuously from those which occurred before the magnetopause reached the simulation boundary.

In Figure 6 the plasmoid has become completely detached from the earth and is moving out of the downstream boundary of the simulation box.

4. MAPPING FROM THE IONOSPHERE TO THE MAGNETOSPHERE

In Figure 7 we present another way of visualizing the changes in the magnetospheric configuration (Refs. 10, 11). In the left column we have reproduced the flow pattern in the equatorial plane while in the right column we have mapped constant longitudes and latitudes along magnetic field lines from the ionosphere to the magnetic equatorial plane. Thus there are two sets of curves in the mapping plots. For one set called constant latitude maps, we have calculated the magnetic field lines at all longitudes starting from a fixed latitude on the earth and have drawn a line connecting the equatorial crossing points. These curves are circles near the earth since the dipole field

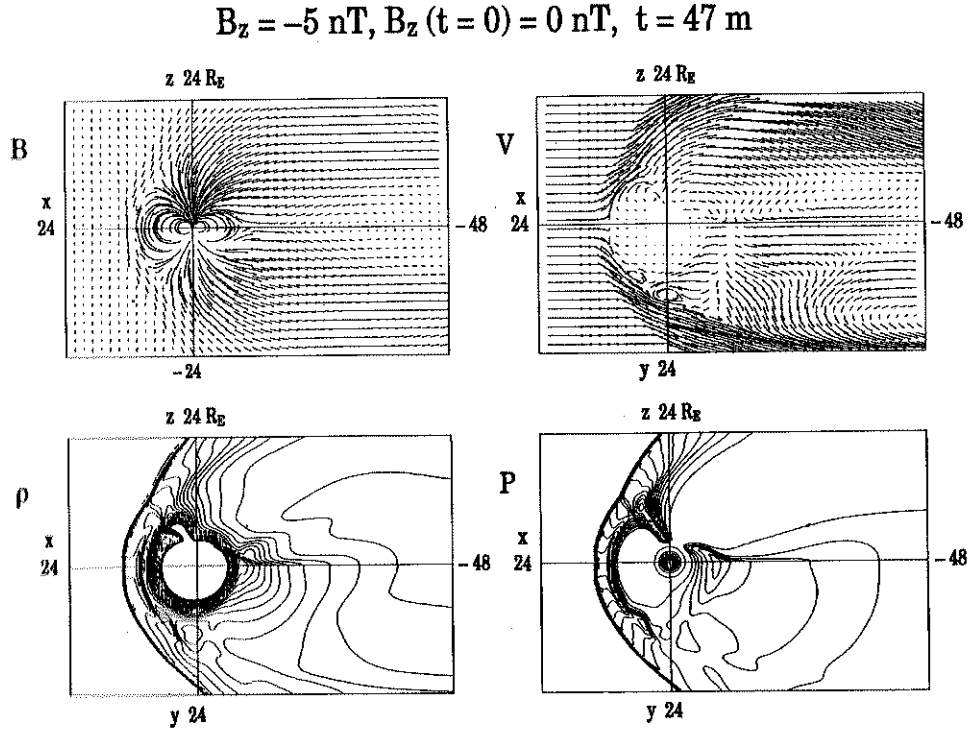

Fig. 3: The same as Figure 1 for $t = 47m$.

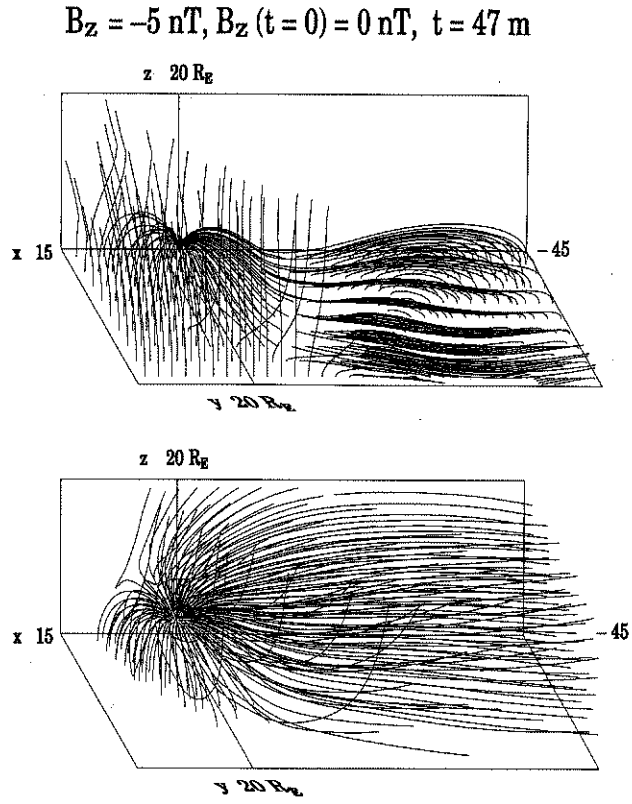

Fig. 4: The same as Figure 2 for $t = 47m$.

dominates there. The higher latitude curves are distorted an extend into the tail. For the second set of curves we kept th local time constant and calculated the field lines for different lat itudes. These constant longitude maps are radial in the dipol field region but bend and become roughly parallel to the sol wind in the tail. The mapping of any point in the ionosphere t the magnetosphere can be determined from the intersection c the corresponding latitude and longitude curves.

At $t = 28m$, which is prior to the onset of tail reconnectio the 70° field line at midnight connects to a point in the equat at about $x \approx -25R_E$ while the 71° field line connects to near the end of the simulation box ($x \approx -45R_E$). Between 28 and 38m the plasma sheet has thinned so that at $t = 38m$ th 70° field line extends to the end of the box. Nearer the ear there is a "hole" in the map. No closed field lines connect to thi region which is occupied by the plasmoid. That the reconnectio starts in a small region near midnight is most clearly seen in thi display. By $t = 47m$ the reconnection has moved across the ta and only a few closed field lines still map to the downstrea boundary. Finally by $t = 57m$ all of the closed field lines hav been reconnected and the "hole" includes the entire magnetota tailward of the x line.

5. MAPPING FROM THE MAGNETOSPHERE TO THE AURORAL IONOSPHERE

The mapping process has been reversed in Figure 8. W call this a local time and radial distance mapping. To genera the local time curves we calculated the ionospheric intercepts field lines starting from fixed local times in the equatorial plan These curves are radial at low latitudes but curve towards noo at higher latitudes. For the radial distance curves we calculat

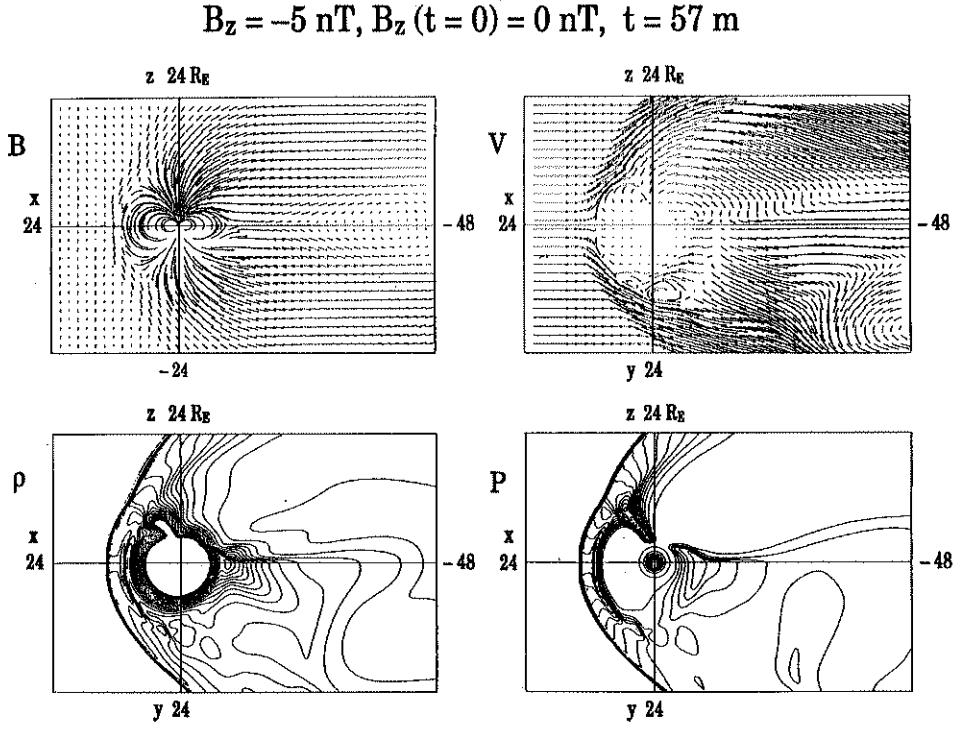

Fig. 5: The same as Figure 1 for $t = 57m$.

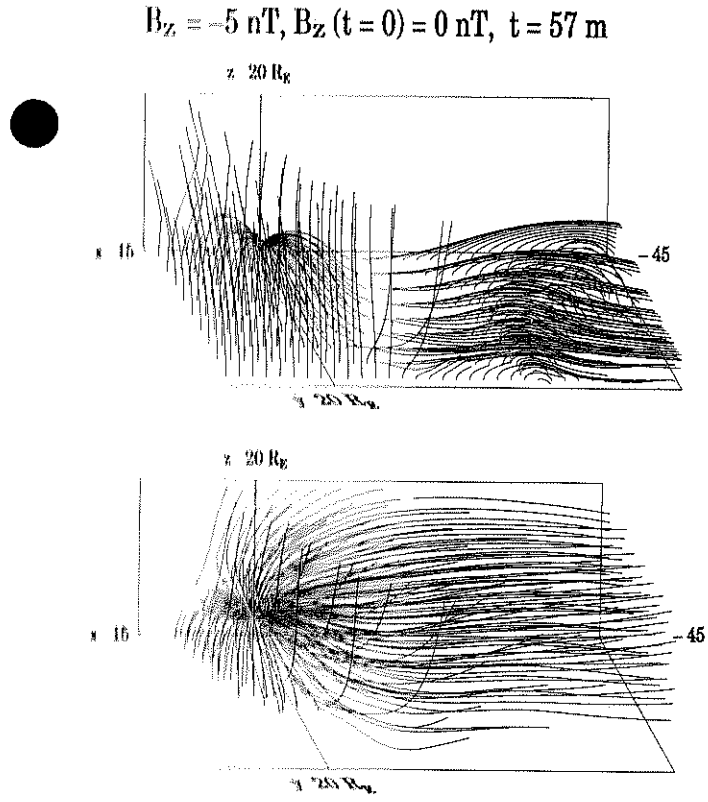

Fig. 6: The same as Figure 2 for $t = 57m$.

the ionospheric field line intercepts keeping the radial distance in the equatorial plane constant. At lower latitudes these curves are nearly circular but become elongated at higher latitudes. Any point in the equatorial magnetosphere can be mapped to the ionosphere by finding the point of intersection of the appropriate curves.

The area within the inner most curve in Figure 8 is the region of the ionosphere that maps to open field lines (the polar cap). In the interval between $t = 28m$ and $t = 57m$ the polar cap has become larger. This occurs because reconnected flux has been added to the tail lobes. At midnight the last closed field line has moved from a latitude of about 72° to about 70°.

In the right panel of Figure 8 we have mapped the energy flux ($\alpha = |(\vec{v}_{th} + \vec{v}_{\parallel})P|$ where $\vec{v}_{th}$ is the thermal velocity and $\vec{v}_{\parallel}$ is the parallel velocity) into the auroral zone. We would expect that the region of enhanced energy flux would most closely approximate the diffuse auroral oval. The contoured region is consistent with the expected auroral oval position and shape. The enhanced energy flux is mainly on closed field lines. However there is appreciable energy flux into the ionosphere from open field lines in the polar cusp region. At midnight there is some energy flux to the ionosphere on open field lines adjacent to the plasma sheet. This is not present after reconnection starts on open field lines.

6. DISCUSSION AND SUMMARY

Our simulation results for southward IMF in general are consistent with the expectations of the near earth neutral line model of substorms. After the southward IMF reaches the dayside magnetopause reconnection begins and magnetic flux is convected into the tail lobes. After about 35m reconnection begins within

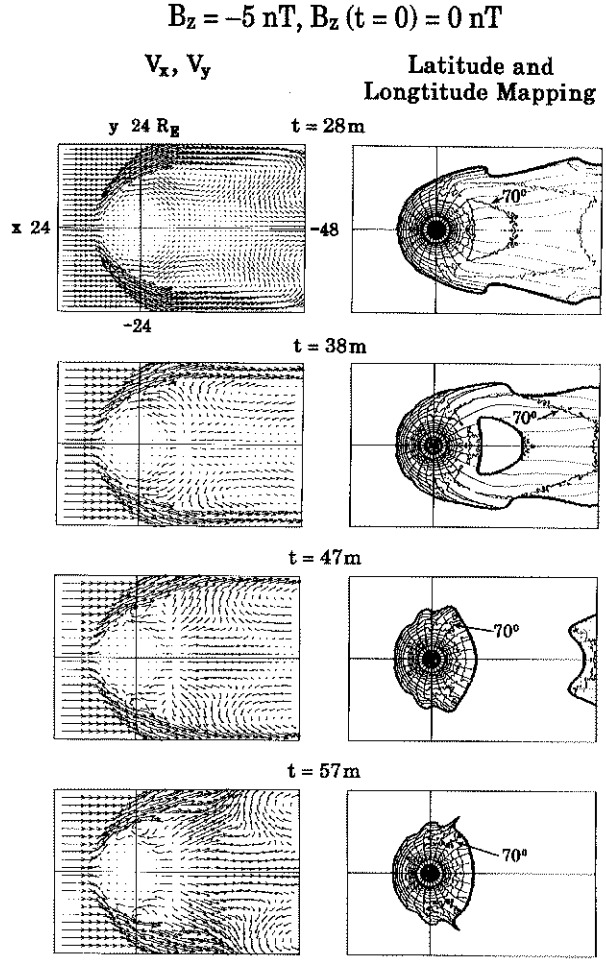

Fig. 7: Flow vectors (Vx, V_y) in the equatorial plane (left) and field line mappings from the ionosphere to the magnetosphere (right) for times 28m, 28m, 47m and 57 m.

the plasma sheet near midnight at $x = -14R_E$. Later the x line moves towards the dawn and dusk magnetopause. When the plasma sheet field lines have reconnected the reconnection begins on lobe field lines freeing the plasmoid to move down the tail under the influence of the tension on reconnected lobe field lines. These results are similar to those we found with an earlier much lower resolution ($\Delta x = 1R_E$) simulation (Ref. 12).

We have modeled magnetospheric dynamics for a number of solar wind velocities and IMF strengths (Ref. 9). For all of our runs the neutral line formed at approximately the same location in the near earth plasma sheet. That location is determined by the energy flux into the tail following the dayside reconnection. During the growth phase the Poynting flux is concentrated in the region where the tail attaches onto the magnetic dipole dominated inner magnetosphere (Ref. 9). For constant solar wind input parameters the delay between the start of the simulation and the onset of reconnection was determined by the size of the normal component B_z of the magnetic field across the equator. Reconnection began after B_z was reduced sufficiently for the tearing mode to grow (Ref. 9).

The results presented here seem to be consistent with the conclusions of some observational studies such as the first CDAW-6 substorm (Ref. 1). However other studies indicate that this is not always the case and that reconnection usually

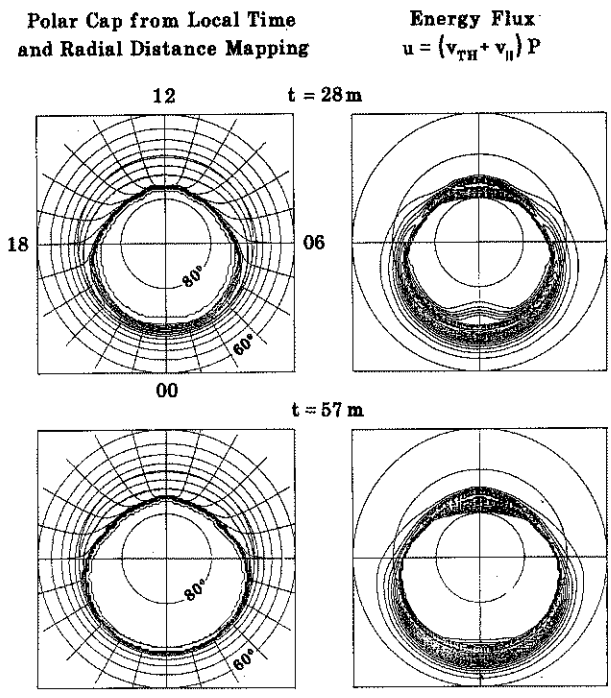

Fig. 8: Field line mappings from the magnetosphere to the ionosphere (left) and the energy flux from the magnetosphere to the ionosphere (right).

occurs tailward of-$20R_E$ (Refs 13 – 15). This remains an area of controversy and intense observational study.

The simulation results do not appear to be consistent with the model that plasma sheet convection is the cause of the near earth neutral line (Refs. 16 - 18). In the simulation most of the flow prior to the onset of reconnection is on the flanks of the magnetosphere near the magnetopause and the earthward convection near midnight is small (Figure 7). This does not appear to be large enough to cause the local minimum in B_z required by the convection theory.

Finally we have begun to use the global MHD simulation to map phenomena along magnetic field lines between the ionosphere and the magnetosphere. The first results are encouraging. The polar cap enlarges for southward IMF as reconnected flux is added to the tail lobes. We have calculated the region of the ionosphere where the energy flux from the magnetosphere is greatest. The energy flux is confined to a region which closely approximates the auroral oval.

So far we have started all of the simulation runs in the same way. A southward IMF enters the simulation box from the upstream boundary and interacts with a dipole magnetic field to form a rapidly evolving magnetosphere. In the real magnetosphere the southward IMF interacts with a magnetosphere which has already formed. In some cases this is a magnetosphere formed by a northward IMF while in others it is the magnetospheric configuration of an ongoing substorm. Our next step in this study will be to carry out a simulation parameter search in which we vary the initial configuration of the simulation.

Another aspect of substorm phenomena not included in our simulation is the recovery phase. In the near earth neutral line model the recovery phase is associated with the tailward retreat of the near earth neutral line. As the neutral line moves tailward the plasma sheet refills behind it. This too awaits further simulation studies.

Acknowledgements. The work at UCLA was supported by NASA Space Physics Theory Program grant NAG5–1480 and the work at Nagoya University was supported by a grant in aid for science research from the Mininstry of Education, Science and Culture.

7. REFERENCES

1. McPherron, R L 1990, Physical processes producing magnetospheric substorms and magnetic storms, *Geomagnetism, 4*, 593.

2. Akasofu, S-I 1981, Energy coupling between the solar wind and the magnetosphere, *Space Sci. Rev., 28*, 121.

3. Akasofu, S.– I 1981, Magnetospheric substorms: A newly emerging model, *Plant. Space Sci., 29*, 10, 1069.

4. Rostoker G & Eastman T ,1987, A boundary layer model for magnetospheric substorms, *J. Geophys. Res., 92* A11, 12187.

5. Smith R A. & al 1986, Thermal catastrophe in the plasma sheet boundary layer, *J. Geophys. Res., 91*, 13, 1380.

6 Goertz, C K & Smith R A 1989, Thermal catastrophe model of substorms, *J. Geophys. Res., 94*, 593.

7. Ogino T & al 1992, A Global Magnetohydrodynamic Simulation of the Magnetosheath and the Magnetosphere When the Interplanetary Magnetic Field is Northward, *IEEE Trans. Plasma Sci.* , submitted.

8. Ogino T 1986, A three dimensional MHD simulation of the interaction of the solar wind with the earth's magnetosphere: The generation of field aligned currents, *J. Geophys. Res., 91* A6, 6791.

9. Walker R J & al 1992, A global magnetohydrodynamic simulation of the magnetosphere when the interplanetary magnetic field is southward: The onset of magnetotail reconnection, *J. Geophys. Res.* submitted.

10. Ogino T & al 1990, Using Global Magnetohydrodynamic Simulations to Map Phenomena from the Magnetosphere to the Polar Ionosphere, (abstract) *EOS Trans. AGU, 71*, 17, 604.

11. Nishitani N & al 1990, The results of magnetospheric magnetic field mapping based on Tsyganenko's magnetic field model, preprint, Solar Terrestrial Environment Laboratory, Nagoya University.

12. Walker R J & al 1988, A global magnetohydrodynamic model of magnetospheric substorms, in *Physics of Space Plasmas, SPI Conf. Proc. Reprint Ser.*, 7, 235.

13. Cattell C A & Mozer F S 1984, Substorm electric fields in the earth's magnetotail, in *Magnetic Reconnection in Space and Laboratory Plasmas, Geophys. Monogr. Ser. 30*, 208.

14. Huang C Y & Frank L A 1986, A statistical study of the central plasma sheet: Implications for substorm models, *Geophys. Res. Lett., 13*, 7, 652.

15. Baumjohann W & al 1989, Average plasma properties in the central plasma sheet, *J. Geophys. Res., 94*, A6, 6597.

16. Erickson G M & Wolf R A 1980, Is steady convection possible in the earth's geomagnetic tail?, *Geophys. Res. Lett., 7*, 897.

17. Erickson G M 1984, On the cause of x-line formation in the near-earth plasma sheet: Results of adiabatic convection of plasma sheet plasma, in *Magnetic Reconnection in Space and Laboratory Plasmas, Geophys. Monogr. Ser. 30*, 296.

18. Hau L-N & al. 1989, Steady state magnetic field configurations for the earth's magnetotail, *J. Geophys. Res., 94*, 1303.